On Multimode Equivalent Network Representation of Finite Arrays of Open-Ended Waveguides

Daniel Sánchez-Escuderos, *Member, IEEE,* Mariano Baquero-Escudero, *Member, IEEE,* Pablo Soto, *Member, IEEE,* Vicente E. Boria, *Senior Member, IEEE,* Marco Guglielmi, *Fellow, IEEE,*

***Abstract*—This paper describes a multimode equivalent network (MEN) representation of a finite array of open-ended lossless waveguides on an infinite ground plane. The derivation is based on an integral equation formulated at the interface between the waveguides and the free-space region. The MEN is formulated using the concept of accessible and localized modes, and includes ports for the free-space plane waves. The MEN derived can be easily combined with the MENs of other microwave components, thus allowing for the accurate analysis and design of more complex systems composed of waveguide elements and radiating apertures. Both simulated and experimental results are presented showing very good agreement, thereby fully validating the proposed equivalent network representation.**

***Index Terms*—Waveguide radiation, integral equation technique, multimode equivalent network representation, plane-wave expansion.**

I. Introduction

Rectangular and circular apertures are commonly used as phased array antennas in microwave and millimeter-wave radars [1], [2], and to feed parabolic reflectors in communications satellites [3].

The radiation from a finite number of apertures in an infinite ground plane is indeed a classic problem that has been studied by many authors. In 1969 Mailloux described the single or double mode radiation from two apertures [4], [5]. The result was an impedance matrix that accounted for the mutual coupling between the different modes. Later, in 1976, Harrington provided a more general formulation for aperture problems based on the method of moments [6]. In 1990, Bird studied the mutual coupling in arrays of apertures with different sizes, giving as a result the mutual admittance between modes in the different waveguides (rectangular [7] or elliptical [8]).

The Multimode Equivalent Network (MEN) formulation was originally developed for periodic metal strip gratings in 1989 [9], and later applied to inductive [10], capacitive [11], and general planar [12] waveguide discontinuities. For the latter case, the concept of accessible and localized modes, formally introduced in [13], was exploited to improve the computational efficiency. The MEN formulation has been used, so far, to study the radiation from an infinite set of open-ended waveguides, and for frequency selective surfaces [14]. Furthermore, in [15], a MEN representation of a finite array of open-ended waveguides on a finite ground plane was indeed presented.

None of the aforementioned MEN representations provide access ports for the free-space modes. However, the industrial design of a complete antenna system may require the integrated design of radiating apertures, reflectors, and the complete feeding network [16], [17], including also the effects of an incident field. In this context, therefore, it becomes important to have MENs for radiating apertures assemblies that allow for the inclusion of ports representing plane waves in the free-space region, in addition to the feeding waveguide modes.

This work was supported by the Spanish Ministry of Economics and competitiveness under projects TEC2013-47360-C3-3-P, TEC2016-79700-C2-1-R, TEC2016-78028-C3-3-P, TEC2013-47037-C5-1-R and TEC2016-75934-C4-1-R, and by Generalitat Valenciana under project GV/2015/065.

D. Sánchez-Escuderos, M. Baquero-Escudero, P. Soto, V. E. Boria and M. Guglielmi are with the Instituto de Telecomunicaciones y Aplicaciones Multimedia (ITEAM) of the Universitat Politècnica de València, c/ Cami de Vera s/n, 46022 Valencia, Spain (e-mail: dasanes1@iteam.upv.es, mbaquero@dcom.upv.es, pabsopac@dcom.upv.es, vboria@dcom.upv.es, marco.guglielmi@iteam.upv.es)

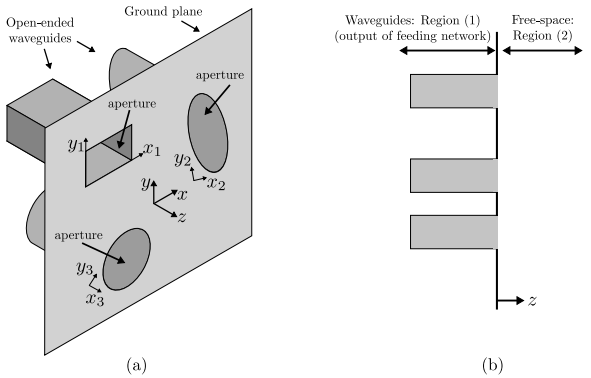

Fig. 1. Generic configuration of 3 radiating, open-ended waveguides: (a) 3D view of the array, and (b) lateral view of considered regions.

A generalized network representation of a finite array of open-ended waveguides on a planar ground plane with free space ports has been already described in [18], [19]. In these contributions, however, the field in the free-space region is expanded in a set of spherical-wave mode functions. This choice, in turns, requires the introduction of an additional "cavity" region, which implies an additional computational effort.

In this paper we derive a MEN representation for an arbitrary array of radiating open-ended waveguides on an infinite ground plane including also network ports for the free-space plane waves. The derivation itself is general and is applicable to any type of lossless waveguide by suitably deriving the transverse wavenumbers of the waveguide and computing the corresponding eigenfunctions [20]. In case of considering canonical waveguides, e.g. rectangular or circular, the efficiency of the MEN representation is maximized. In addition to theory, a number of comparisons between measured and simulated results is also included. Excellent agreement between measurements and simulations is demonstrated, thereby fully validating the proposed multimode equivalent network representation.

II. Problem and Modes definition

The problem under investigation is an arbitrary number of open-ended waveguides on an infinite ground plane. For the sake of simplicity, we show in Fig. 1 an example with only three radiating open-ended waveguides.

As shown in Fig. 1 (b), the structure is divided into two regions: Region (1), composed of T waveguides, and Region (2), the free-space region. The objective of this paper is to develop a multimode equivalent network (MEN) representation for the structure in Fig. 1 in the form shown in Fig. 2. The MEN shown in Fig. 2 is similar to the MENs first introduced in [9]-[12] for modelling waveguide obstacles, with two important differences. First, the ports in region (2) denote free-space plane waves instead of waveguide modes. Second, the proposed representation does not add a static admittance (or impedance) in parallel (or in series) to each of the transmission lines representing the modes connected to the MEN matrix. The removal of these static terms results in a simpler network formalism that increases the computational efficiency. The improvement in computational efficiency may be small for each single mode, but may become significant when complex structures, with a large number of accessible modes, are analyzed and optimized. This aspect, however, goes beyond the scope of the present work and will be fully explored in future research activities.

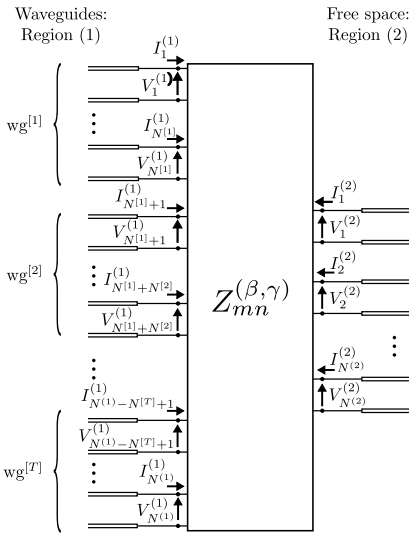

Fig. 2. Multimode equivalent network for the structure in Fig. 1.

To start our formulation we write the electromagnetic fields in region (1) as [21]:

$$\boldsymbol{E}_t^{(1)}(x,y,z) = \sum_{p=1}^{\infty} V_p^{(1)}(z)\boldsymbol{e}_p{}^{(1)}(x,y) \tag{1}$$

$$\boldsymbol{H}_t^{(1)}(x,y,z) = \sum_{p=1}^{\infty} I_p^{(1)}(z)\boldsymbol{h}_p{}^{(1)}(x,y) \tag{2}$$

where $V_p^{(1)}(z)$ and $I_p^{(1)}(z)$ are the modal voltages and currents of the modal expansion, and $\boldsymbol{e}_p{}^{(1)}(x,y)$ and $\boldsymbol{h}_p{}^{(1)}(x,y)$ are the normalized electric and magnetic vector functions for the waveguides modes corresponding to region (1). The index p summarizes in a single notation the mode index (m,n), and the TE or TM mode type associated to each waveguide τ ($\tau = 1 \dots T$ in our structure).

Region (2), representing the free space, may also be considered as a uniform waveguide having an infinite cross section (x and y directions), with propagation in the z direction [21]. From this point of view, therefore, the electromagnetic fields in free space may also be written with a modal formalism that is similar to the one of closed waveguides. The difference, however, is that the modal spectrum for the free-space region is continuous instead of discrete. The expressions for the transverse electric and magnetic fields in region (2) can therefore be written as follows:

$$\boldsymbol{E}_t^{(2)}(x,y,z) = \int_{-\infty}^{\infty}\int_{-\infty}^{\infty} V_i^{(2)}(z)\boldsymbol{e}_i{}^{(2)}(x,y)\mathrm{d}k_x\mathrm{d}k_y \tag{3}$$

$$\boldsymbol{H}_t^{(2)}(x,y,z) = \int_{-\infty}^{\infty}\int_{-\infty}^{\infty} I_i^{(2)}(z)\boldsymbol{h}_i{}^{(2)}(x,y)\mathrm{d}k_x\mathrm{d}k_y \tag{4}$$

where $V_i^{(2)}(z)$ and $I_i^{(2)}(z)$ are the modal voltages and currents of the plane-wave expansion, and $\boldsymbol{e}_i{}^{(2)}(x,y)$ and $\boldsymbol{h}_i{}^{(2)}(x,y)$ are the normalized electric and magnetic vector mode functions in the free-space region, respectively. The index i summarizes in a single term the free-space spectral wavenumber (k_x,k_y), which may also be TE or TM.

The far-field radiation pattern of the apertures ($\boldsymbol{E}_{FF}$) can be computed from (3) and (4) by solving the integrals with the method of the stationary phase [22, Appendix VIII]. The result can be expressed as:

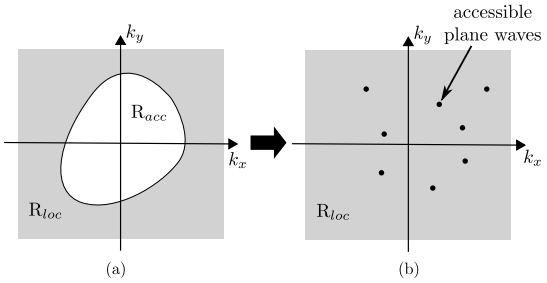

Fig. 3. Region (2) integration limits: (a) accessible R_{acc} and localized R_{loc} regions, and (b) set of plane waves within R_{loc}.

$$\boldsymbol{E}_{FF}(r,\theta,\phi) = jk\frac{e^{-jkr}}{r}(V_i^{(\mathrm{TM})\ (2)}\hat{\theta} - \cos\theta V_i^{(\mathrm{TE})\ (2)}\hat{\phi}), \tag{5}$$

where the modal voltages are split into TE and TM modes, and the relationship between the direction (θ,ϕ) and the index $i \equiv (k_x,k_y)$ is given by $k_x = k\sin\theta\cos\phi$ and $k_y = k\sin\theta\sin\phi$, where k is the wavenumber.

The explicit expressions for the orthonormal mode functions in the waveguides region and in the free-space region can be found in [21, Ch. 2].

III. Integral equation technique

The first step in the formulation is to write the transversal magnetic field in the waveguide region in the following form:

$$\boldsymbol{H}_t^{(1)}(x,y,z) = \sum_{p=1}^{N^{(1)}} I_p^{(1)}(z)\boldsymbol{h}_p{}^{(1)}(x,y) + \sum_{p=N^{(1)}+1}^{\infty} I_p^{(1)}(z)\boldsymbol{h}_p{}^{(1)}(x,y) \tag{6}$$

where the concept of *accessible* modes (those that interact with other junctions) and *localized* modes (those that are relevant in the characterization of the aperture, but do not contribute to the interactions with other junctions) has been used [13], so that $N^{(1)}$ is the number of accessible modes in all waveguides.

The same separation can also be introduced in region (2). However, accessible and localized modes are now located in different 2D spectral regions: R_{acc} for accessible modes, and R_{loc} for localized modes, as illustrated in Fig. 3 (a). Consequently, the transverse magnetic vector field for region (2) is written as follows:

$$\boldsymbol{H}_t^{(2)}(x,y,z) = \iint_{\mathrm{R}_{acc}} I_i^{(2)}(z)\boldsymbol{h}_i{}^{(2)}(x,y)\mathrm{d}k_x\mathrm{d}k_y + \iint_{\mathrm{R}_{loc}} I_i^{(2)}(z)\boldsymbol{h}_i{}^{(2)}(x,y)\mathrm{d}k_x\mathrm{d}k_y. \tag{7}$$

However, in the case in which we are only interested in a set of *accessible* plane waves, as illustrated in Fig. 3 (b), (7) can be rewritten as:

$$\boldsymbol{H}_t^{(2)}(x,y,z) = \sum_{i=1}^{N^{(2)}} I_i^{(2)}(z)\boldsymbol{h}_i{}^{(2)}(x,y) + \iint_{\mathrm{R}_{loc}} I_i^{(2)}(z)\boldsymbol{h}_i{}^{(2)}(x,y)\mathrm{d}k_x\mathrm{d}k_y \tag{8}$$

where $N^{(2)}$ is the number of accessible planes waves, and R_{loc} now covers the complete spectral domain. The location of the accessible plane waves (k_x,k_y) is directly determined from the spatial directions (θ,ϕ) in which the radiation pattern must be computed, as stated above. Note that the accessible plane waves are discrete points whose area is null. Thereby, R_{loc} in (8) can be extended to the whole plane-wave spectrum domain without altering the final result.

To continue, we note now that the apertures are located at $z = 0$ and, therefore, voltages and currents for the localized modes can be simplified to:

$$I_n^{(\gamma)} = -I_n^{(\gamma)-} = -Y_n^{(\gamma)} V_n^{(\gamma)} \tag{9}$$

where (γ) indicates region (1) or (2), and $Y_n^{(\gamma)}$ are the modal admittances and $I_n^{(\gamma)-}$ the reflected waves.

Taking into account the formalism introduced, we can now write the following expression for the continuity of the transversal magnetic fields at $z = 0$:

$$\sum_{p=1}^{N^{(1)}} I_p^{(1)} \boldsymbol{h}_p^{(1)}(x,y) - \sum_{p=N^{(1)}+1}^{\infty} Y_p^{(1)} V_p^{(1)} \boldsymbol{h}_p^{(1)}(x,y) = \\ - \sum_{i=1}^{N^{(2)}} I_i^{(2)} \boldsymbol{h}_i^{(2)}(x,y) + \iint_{\mathrm{R}_{loc}} Y_i^{(2)} V_i^{(2)} \boldsymbol{h}_i^{(2)}(x,y) \mathrm{d}k_x \mathrm{d}k_y, \tag{10}$$

where the modal voltages for regions (1) and (2) may be expressed as:

$$V_n^{(\gamma)} = \iint_{S_\gamma} \left(\hat{z} \times \boldsymbol{E}_t(x',y') \right) \boldsymbol{h}_n^{(\gamma)*}(x',y') \mathrm{d}S' \tag{11}$$

being $\hat{z} \times \boldsymbol{E}_t(x',y')$ the unknown of the problem under investigation, S_1 the cross-section of waveguide τ associated to mode n, and S_2 the union of all the aperture cross-sections (S_T).

Introducing (11) into (10), $\hat{z} \times \boldsymbol{E}_t(x',y')$ is now expressed in terms of an integral equation. Note, however, that since the problem is linear, $\hat{z} \times \boldsymbol{E}_t(x',y')$ can be written as a linear combination of accessible modes in both regions. Furthermore, defining a new set of magnetic-current functions ($\boldsymbol{M}_q^{(1,2)}(x',y')$) as the unknown of the problem, we can write the transverse electric field at $z = 0$ in the form:

$$\hat{z} \times \boldsymbol{E}_t(x',y') = \sum_{q=1}^{N^{(1)}} I_q^{(1)} \boldsymbol{M}_q^{(1)}(x',y') + \sum_{j=1}^{N^{(2)}} I_j^{(2)} \boldsymbol{M}_j^{(2)}(x',y'). \tag{12}$$

Using now (11), and (12), in (10), and equating like terms, we can obtain a set of integral equations for the unknown magnetic-current functions:

$$\boldsymbol{h}_n^{(\gamma)}(x,y) = \\ \iint_{S_T} \boldsymbol{M}_n^{(\gamma)}(x',y') \left[\sum_{q=N^{(1)}+1}^{\infty} Y_q^{(1)} \boldsymbol{h}_q^{(1)}(x,y) \boldsymbol{h}_q^{(1)*}(x',y') + \right. \\ \left. \iint_{\mathrm{R}_{loc}} Y_j^{(2)} \boldsymbol{h}_j^{(2)}(x,y) \boldsymbol{h}_j^{(2)*}(x',y') \mathrm{d}k_x \mathrm{d}k_y \right] \mathrm{d}S' \tag{13}$$

where n indicates any accessible mode of regions (1) or (2).

Once the integral equation is solved, the impedance matrix $Z_{mn}^{(\beta,\gamma)}$ can be computed by substituting the magnetic-current $\boldsymbol{M}_q^{(\gamma)}(x',y')$ into (11). The resulting final expression is as follows:

$$Z_{mn}^{(\beta,\gamma)} = \iint_{S_T} \boldsymbol{M}_n^{(\gamma)}(x',y') \boldsymbol{h}_m^{(\beta)*}(x',y') \mathrm{d}S' \tag{14}$$

where β and γ denote the region (1 or 2) to which modes m and n belong, respectively, and where the impedance matrix elements in (14) relate the modal voltages and currents as follows:

$$V_m^{(\beta)} = \sum_{n=1}^{N^{(1)}} I_n^{(1)} Z_{mn}^{(\beta,1)} + \sum_{n=1}^{N^{(2)}} I_n^{(2)} Z_{mn}^{(\beta,2)}. \tag{15}$$

IV. Solution of the integral equation: Multimode equivalent network representation

The set of integral equations in (13) can be solved using the method of moments [23]. To do so, the unknown magnetic-currents $\boldsymbol{M}_n^{(\gamma)}(x',y')$ in the apertures are expanded as a series of magnetic basis functions in region (1) as follows:

$$\boldsymbol{M}_n^{(\gamma)}(x',y') = \sum_{q=1}^{Q^{(\gamma)}} \alpha_q^{(n,\gamma)} \boldsymbol{h}_q^{(1)}(x',y') \tag{16}$$

being the coefficients of this expansion ($\alpha_q^{(n,\gamma)}$) the unknowns of the problem. Using Galerkin's Method [23] in (13) we then obtain:

$$B_{pq} \alpha_q^{(n,\gamma)} = C_p^{(n,\gamma)} \tag{17}$$

where the system matrix and the independent vector are defined as:

$$B_{pq} = Y_q^{(1)} F_q \delta_{pq} + I_{pq} \tag{18}$$

$$C_p^{(n,\gamma)} = \begin{cases} \delta_{np}, & \text{if } \gamma = 1 \\ A_{np}, & \text{if } \gamma = 2 \end{cases} \tag{19}$$

with

$$I_{pq} = \iint_{\mathrm{R}_{loc}} Y_i^{(2)} A_{iq}^* A_{ip} \mathrm{d}k_x \mathrm{d}k_y, \tag{20}$$

and where $Y_i^{(2)}$ is the admittance of the free-space mode i, and F_q is 0 for accessible modes and 1 for localized modes. The coupling integral A_{np} is defined as:

$$A_{np} = \iint_{S_p} \boldsymbol{h}_n^{(2)}(x,y) \cdot \boldsymbol{h}_p^{(1)*}(x,y) \mathrm{d}S, \tag{21}$$

being S_p the transverse area of the waveguide associated to mode p.

By solving (17), the weights of the expansion ($\alpha_q^{(n,\gamma)}$) are determined and, with these weights, the unknown magnetic basis functions $\boldsymbol{M}_n^{(\gamma)}(x',y')$ can be easily obtained through (16). These functions can be used, in turn, to compute the elements of the impedance matrix using (14), so that:

$$Z_{mn}^{(\beta,\gamma)} = \begin{cases} \alpha_m^{(n,\gamma)}, & \text{if } \beta = 1 \\ \displaystyle\sum_{q=1}^{Q^{(\gamma)}} \alpha_q^{(n,\gamma)} A_{mq}^*, & \text{if } \beta = 2. \end{cases} \tag{22}$$

V. Experimental results

In this section we present several results to validate the MEN derived, which has been implemented using the FORTRAN programming language. For the sake of simplicity, we will use rectangular radiating apertures. It is also important to stress that, in contrast to previous MENs formulations (such as [15]), which requires additional far field projections, the method described in this paper is able to provide directly the radiation pattern as the voltages of the modes (i.e., plane waves) in region (2) can be obtained.

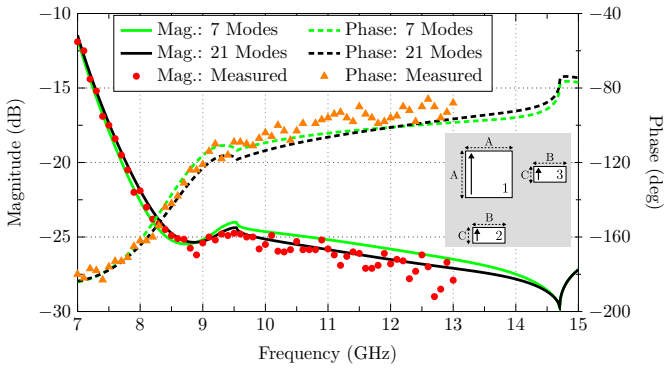

Fig. 4. S_{11} parameter in the square (central) aperture of the three-aperture array shown in the inset. Measurements are from [7].

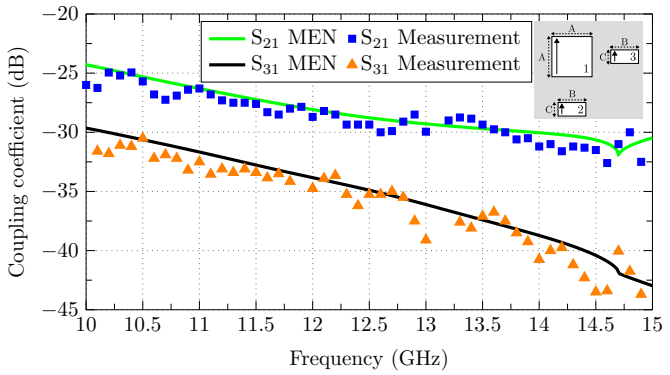

Fig. 5. Coupling coefficient between aperture 1 and apertures 2 and 3 (see the inset) with 21 modes on each aperture. Measurements are from [7].

A. Three apertures configuration

The MEN derived has been tested first with the configuration introduced in [7], where measured results of a fabricated prototype were also included for comparison. The structure, shown in the inset of Fig. 4, is formed by three apertures on an infinite ground plane. The central element is a square aperture with side A=22.8 mm, whereas the other elements are rectangular apertures with dimensions B=15.7 mm and C=7.7 mm. The separation between apertures (center to center) is 30 mm.

The structure has been simulated with 7 and 21 magnetic basis functions on the apertures ($Q^{(\gamma)}$ in (16)). The S_{11} parameter of the central square aperture is compared to the measured result extracted from [7] in Fig. 4. Whereas the result with 7 modes is quite similar to the simulated parameter given in [7], the 21-modes solution is more similar to the measured S_{11} parameter since convergence has been reached within the frequency band of interest. Observe that a preliminary convergence study is always mandatory in order to guarantee the correctness of the result.

Fig. 5 shows the mutual coupling between the central element and the rectangular apertures with 21 modes on each aperture (see labels inside each aperture to identify each S parameter). Again, measured and simulated results coincide over the whole frequency range.

The radiation pattern of the structure on the 45° plane has also been calculated at 12.5 GHz. To do so, only the square aperture has been fed, whereas the rest of apertures have been terminated with a matched load. The copolar (vertical) and crosspolar (horizontal) components obtained on the 45° plane (MEN) are compared in Fig. 6 to the pattern simulated with HFSS [24]. A very good agreement between both simulated results can be observed, thereby verifiyng the proposed MEN formulation.

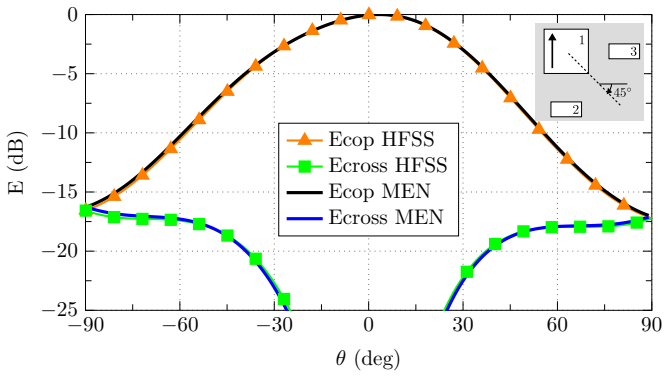

Fig. 6. Radiation pattern of the 3-apertures configuration on the 45° plane at 12.5 GHz when only aperture 1 is fed (see inset) and 21 modes on each aperture are considered.

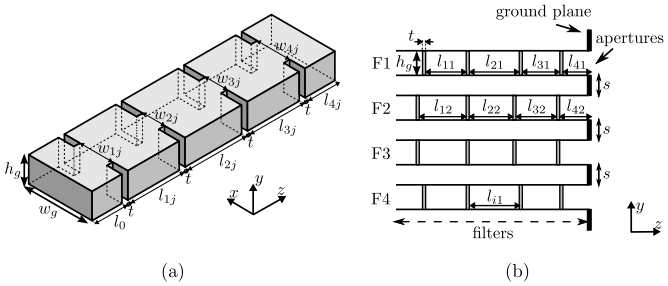

Fig. 7. Open-ended waveguide filters with inductive irises: (a) isolated 3D view of a filter, and (b) lateral view of the four filters.

B. Open-ended waveguide filters

Even though the previous example fully confirms the validity of the new MEN formulation, the usefulness of the method can only be tested with a more complex example. To this aim, we present in this section the results for a structure formed by four 3-pole filters with the last waveguide section radiating in the free-space region.

Fig. 7 (a) shows a sketch of an isolated filter composed of sections of rectangular waveguides coupled to each other by inductive irises. The dimensions of all the rectangular waveguide sections are: w_g =10.668 mm and h_g =4.318 mm, and the thickness of all the inductive irises is t =1 mm. Only the length of the waveguide sections (l_{ij}) and the width of the inductive irises (w_{ij}) have been optimized to get the desired filtering response.

The optimization has been carried out by considering all four filters simultaneously to account for the mutual coupling between the apertures. The filters are set along the y axis, as shown in Fig. 7 (b), with a separation of s = 7 mm. The central filters (F2 and F3) and the outer filters (F1 and F4) have the same dimensions. The filters have been optimized to have a return loss better than 20 dB between 19.75 GHz and 20.25 GHz. The obtained dimensions for F1 and F2 are: l_{11}=8.708 mm, l_{21}=9.541 mm, l_{31}=8.914 mm, l_{41}=1.991 mm, l_{12}=8.709 mm, l_{22}=9.535 mm, l_{32}=8.902 mm, l_{42}=1.982 mm, w_{11}=5.521 mm, w_{21}=3.691 mm, w_{31}=3.694 mm, w_{41}=5.070 mm, w_{12}=5.515 mm, w_{22}=3.693 mm, w_{32}=3.703 mm and w_{42}=5.065 mm.

The same structure has been simulated with HFSS [24] to verify the accuracy of the results. For this example we have used 300 basis functions and 100 accessible modes in the apertures and in the filter interfaces. This combination gives an error in the S parameters below 0.01 dB. A meshing with a similar threshold for the S parameters has been used for the HFSS simulations.

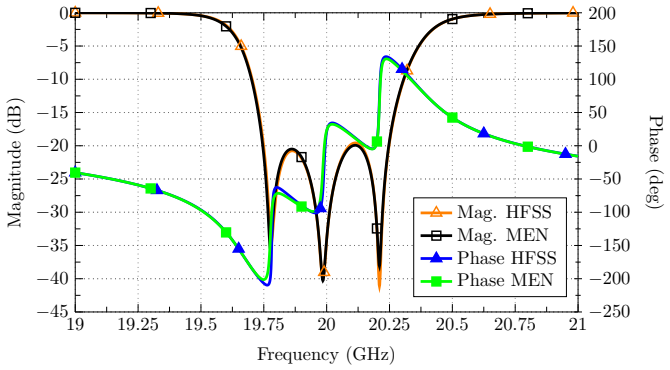

Fig. 8. S_{11} parameter at any input port of the four open-ended filters with inductive irises.

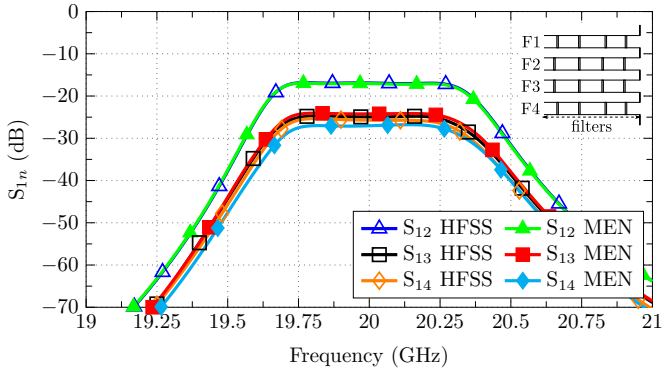

Fig. 9. Mutual coupling between different the input ports of the four open-ended filters with inductive irises.

Fig. 8 compares the S_{11} parameter computed with our MEN and the one obtained using HFSS. Note that only one reflection parameter is shown, since all filters have been optimized to have the same response. This comparison shows good agreement between both simulations, especially in the position of the reflection zeros.

The mutual coupling between filter F1 and filters F2, F3 and F4 is shown in Fig. 9. The S_{12} and the S_{13} parameters match the HFSS response quite well. However, the discrepancy in the S_{14} parameter between the MEN and HFSS is caused by the treatment of the infinite ground plane in HFSS that is known to have some computational limitations.

The directivity of the four-filters configuration on the XZ and YZ planes at 20 GHz is shown in Fig. 10. To obtain this pattern, all filters have been fed with the same amplitude and phase. As can be observed, the MEN results and the HFSS results agree quite well. Again, the non-perfect characterization of the infinite ground plane in HFSS slightly alters the results, giving a small difference at high visibility angles ($\theta > 75°$).

The computation time of the complete four-filters structure using the MEN derived is 0.5 s per frequency point. The simulation in HFSS with the required accuracy took 3 minutes per frequency. In both cases, the computer used had an Intel® Core™ i7-4790K@4.00GHz processor and 32 GB of RAM memory. A considerable improvement in the computation time has been clearly achieved. It is important to note also that this result clearly shows the efficiency of the MEN formulation for the analysis and optimization of complex antenna systems composed of several waveguide components, and radiating apertures. In this case, in fact, the MEN formulation is about two order of magnitude faster than commercial software.

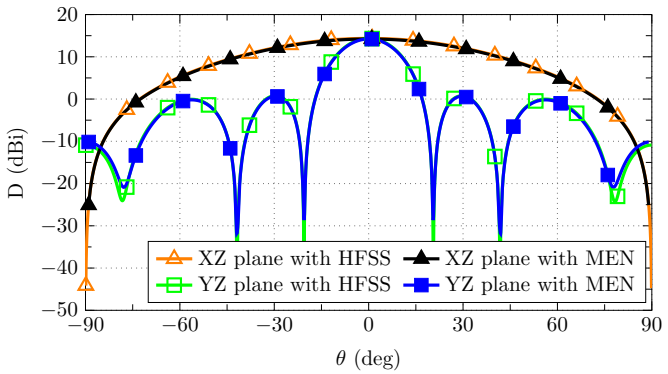

Fig. 10. Directivity of the four open-ended filters with inductive irises on the XZ and YZ planes at 20 GHz. All filters are fed with the same amplitude and phase.

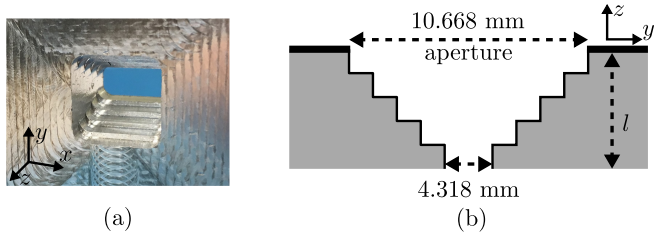

Fig. 11. Discrete-step horn antenna: (a) picture of the prototype, and (b) side view sketch.

C. Discrete-step horn antenna

The MEN formulation proposed is also suitable for simulating horn antennas composed of a number of waveguide sections. Fig. 11 (a) shows a horn antenna formed by 5 waveguides that sequentially open from a WR-42 waveguide (with dimensions 10.668×4.318 mm^2) to a square aperture with dimensions 10.668×10.668 mm^2.

Fig. 11 (b) shows a side view of the horn. Two prototypes have been fabricated, one with a length l =10 mm, and another one with a length l =15 mm. In both cases, the size of the ground plane is 11.5×11.5 mm^2. The corners of the different waveguides that form the horn have a radius of 1.5 mm.

The S_{11} parameter for both configurations (l =10 mm and l =15 mm) is shown in Fig. 12 (Magnitude) and Fig. 13 (Phase). In both cases, the experimental (MEAS) and simulated results (MEN) agree quite well. It is worth noting that the MEN computation takes 0.8 s per frequency (including the time required to compute the modal spectrum of rectangular waveguides with rounded corners), whereas the simulation in HFSS (considering the same accuracy in both cases) takes 30 s per frequency.

The radiation pattern of the longer horn (l =15 mm) has been also measured and simulated at 20.45 GHz. Fig. 14 compares both results and, as can be observed, a good matching between both patterns is obtained. Note that oscillations in the measured prototype are caused by the finite size of the ground plane.

VI. Conclusion

In this paper we present a new formulation for the characterization of open-ended waveguides based on a multimode equivalent network (MEN) representation. The most important advantage of the formulation proposed lies in the fact that the MEN obtained is fully compatible with the network representation of other waveguide junctions. As a result, more complex structures composed of power dividers, filters, and other passive devices connected to radiating

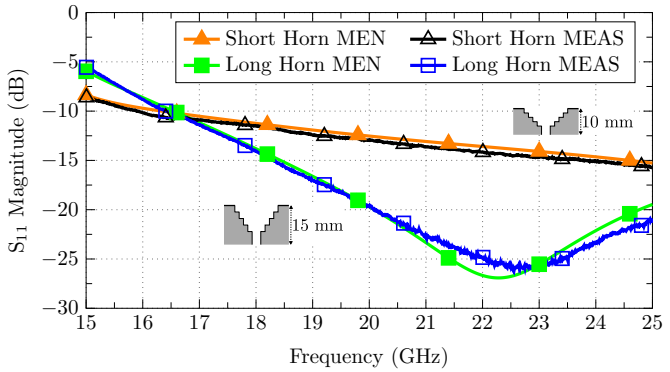

Fig. 12. Magnitude of the S_{11} parameter of the discrete-step horn antenna with two different lengths and the same aperture size (10.668×10.668 mm^2).

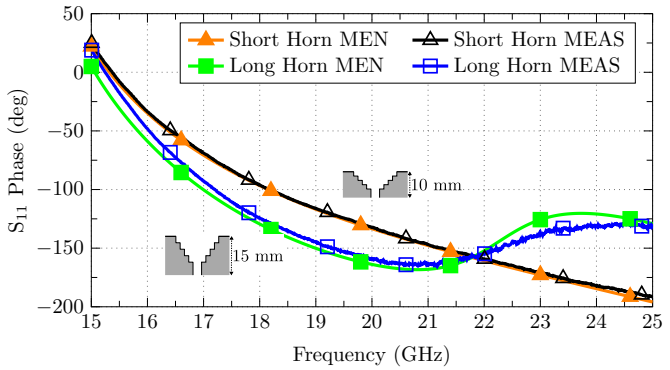

Fig. 13. Phase of the S_{11} parameter of the discrete-step horn antenna with two different lengths and the same aperture size (10.668×10.668 mm^2).

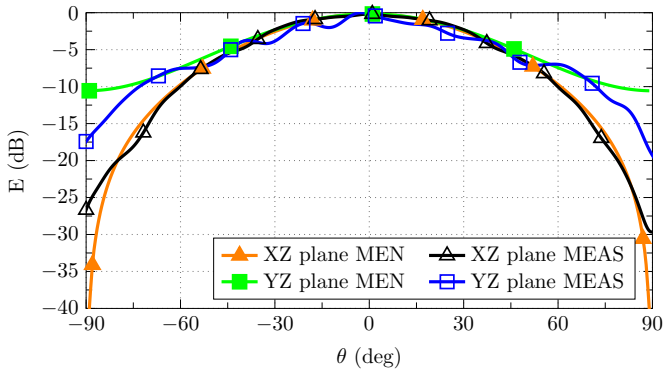

Fig. 14. Radiation pattern on main planes of the long discrete-step horn antenna at 20.45 GHz.

apertures can be easily analyzed and optimized as a whole, thereby simplifying considerably the engineering design task.

Furthermore, the MEN provides explicit access to the free-space modes, and this facilitates the determination of the far-field radiation pattern. In addition, the MEN can also be connected to other MENs through the free-space port to include in the global simulation other structures in free space like reflectors or polarising grids.

Examples shown in this paper fully confirm the validity of the formulation proposed, showing also a considerable reduction of the computation time with respect to commercial software.

The main application of the proposed formulation is in the design of complete antenna systems. Future work is planned for the use of the MEN representation for the analysis and optimization of complete front end of modern microwave systems for both ground and space applications.

REFERENCES

[1] M. I. Skolnik, *Radar handbook*. New York: McGraw-Hill, 1990.
[2] R. C. Hansen, *Phased array antennas*. John Wiley & Sons, 2009.
[3] S. K. Rao, "Advanced antenna technologies for satellite communications payloads," *IEEE Transactions on Antennas and Propagation*, vol. 63, no. 4, pp. 1205–1217, 2015.
[4] R. J. Mailloux, "Radiation and near-field coupling between two collinear open-ended waveguides," *IEEE Transactions on Antennas and Propagation*, vol. 17, no. 1, pp. 49–55, 1969.
[5] ——, "First-order solutions for mutual coupling between waveguides which propagate two orthogonal modes," *IEEE Transactions on Antennas and Propagation*, vol. 17, no. 6, pp. 740–746, 1969.
[6] R. F. Harrington and J. R. Mautz, "A generalized network formulation for aperture problems," *IEEE Transactions on Antennas and Propagation*, vol. 24, no. 6, pp. 870–873, 1976.
[7] T. S. Bird, "Analysis of mutual coupling in finite arrays of different-sized rectangular waveguides," *IEEE Transactions on Antennas and Propagation*, vol. 38, no. 2, pp. 166–172, 1990.
[8] ——, "Behaviour of multiple elliptical waveguides opening into a ground plane," *IEE Proceedings Microwaves, Antennas and Propagation*, vol. 137, no. 2, pp. 121–126, 1990.
[9] M. Guglielmi and A. A. Oliner, "Multimode network description of a planar periodic metal-strip grating at a dielectric interface. I. rigorous network formulations," *IEEE Transactions on Microwave Theory and Techniques*, vol. 37, no. 3, pp. 534–541, 1989.
[10] M. Guglielmi and C. Newport, "Rigorous, multimode equivalent network representation of inductive discontinuities," *IEEE Transactions on Microwave Theory and Techniques*, vol. 38, no. 11, pp. 1651–1659, 1990.
[11] M. Guglielmi and G. Gheri, "Rigorous multimode network representation of capacitive steps," *IEEE Transactions on Microwave Theory and Techniques*, vol. 42, no. 4, pp. 622–628, 1994.
[12] G. Gerini and M. Guglielmi, "Efficient integral equation formulations for admittance or impedance representation of planar waveguide junctions," in *1998 IEEE MTT-S International Microwave Symposium Digest*, vol. 3, 1998, pp. 1747–1750.
[13] T. E. Rozzi and W. F. G. Mecklenbrauker, "Wide-band network modeling of interacting inductive irises and steps," *IEEE Transactions on Microwave Theory and Techniques*, vol. 23, no. 2, pp. 235–245, 1975.
[14] H. J. Visser and M. Guglielmi, "CAD of waveguide array antennas based on "filter" concepts," *IEEE Transactions on Antennas and Propagation*, vol. 47, no. 3, pp. 542–548, 1999.
[15] A. Neto, R. Bolt, G. Gerini, and D. Schmitt, "A multimode equivalent network approach for the analysis of a 'realistic' finite array of open ended waveguides," in *Proc. of 33rd European Microwave Conference*, 2003, pp. 1079–1082.
[16] M. Schneider, C. Hartwanger, and H. Wolf, "Antennas for multiple spot beam satellites," *CEAS Space Journal*, vol. 2, no. 1-4, pp. 59–66, 2011.
[17] J. M. Montero, A. M. Ocampo, and N. J. Fonseca, "C-band multiple beam antennas for communication satellites," *IEEE Transactions on Antennas and Propagation*, vol. 63, no. 4, pp. 1263–1275, 2015.
[18] M. Mongiardo, C. Tomassoni, and P. Russer, "Generalized network formulation: Application to flange mounted radiating waveguides," *IEEE Transactions on Antennas and Propagation*, vol. 55, no. 6, pp. 1667–1678, 2007.
[19] C. Tomassoni, M. Mongiardo, P. Russer, and R. Sorrentino, "Electromagnetic and network theory of waveguide radiation by spherical modes expansions," in *Electromagnetics and Network Theory and their Microwave Technology Applications*. Springer, 2011, pp. 21–34.
[20] S. Cogollos, S. Marini, V. E. Boria, P. Soto, A. Vidal, H. Esteban, J. V. Morro, and B. Gimeno, "Efficient modal analysis of arbitrarily shaped waveguides composed of linear, circular, and elliptical arcs using the bi-rme method," *IEEE Transactions on Microwave Theory and Techniques*, vol. 51, no. 12, pp. 2378–2390, 2003.
[21] N. Marcuvitz, *Waveguide handbook*. Institution of Engineering and Technology, 1986.
[22] C. A. Balanis, *Antenna Theory: Analysis and design.* John Wiley & Sons, 1997.
[23] R. F. Harrington, *Field Computation by Moment Methods*. John Wiley & Sons, 1993.
[24] Ansys Corporation, "HFSS (high frequency structural simulator)," 2014, Suite v15, Pittsburg (PA), USA.